

2012

Evaluation on Heat Pump Cycle Considering Heat Transfer Degradation of Mixture Refrigerant

Yamato Eshima
miyara@me.saga-u.ac.jp

Yoji Onaka

Akio Miyara

Follow this and additional works at: <http://docs.lib.purdue.edu/iracc>

Eshima, Yamato; Onaka, Yoji; and Miyara, Akio, "Evaluation on Heat Pump Cycle Considering Heat Transfer Degradation of Mixture Refrigerant" (2012). *International Refrigeration and Air Conditioning Conference*. Paper 1297.
<http://docs.lib.purdue.edu/iracc/1297>

This document has been made available through Purdue e-Pubs, a service of the Purdue University Libraries. Please contact epubs@purdue.edu for additional information.

Complete proceedings may be acquired in print and on CD-ROM directly from the Ray W. Herrick Laboratories at <https://engineering.purdue.edu/Herrick/Events/orderlit.html>

Evaluation on Heat Pump Cycle Considering Heat Transfer Degradation of Mixture Refrigerant

Yamato ESHIMA¹, Yoji ONAKA¹, Akio MIYARA^{1*}

¹Saga University, Department of Mechanical Engineering,
Saga, Japan

(Phone +81-952-28-8623, Fax +81-952-28-8587, E-mail miyara@me.saga-u.ac.jp)

* Corresponding Author

ABSTRACT

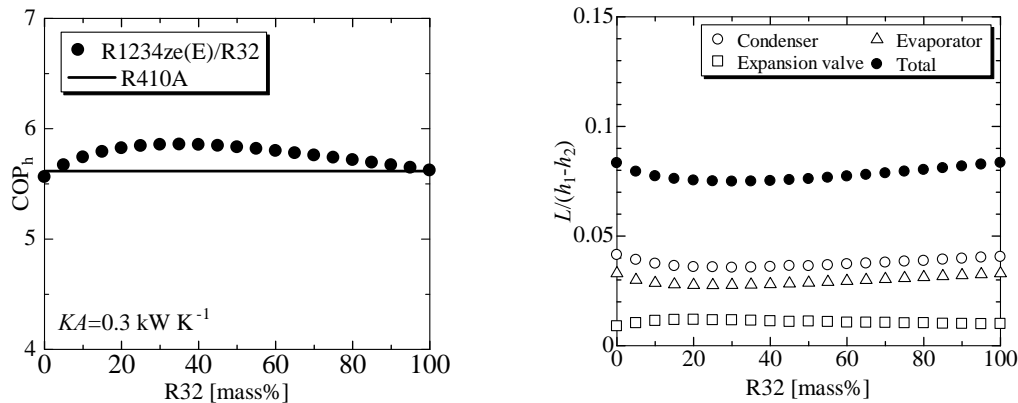
A low GWP refrigerant R1234ze(E) is focused as a candidate of next-generation refrigerant though it has some defects which are low operating pressure and low latent heat. Mixing R32 into R1234ze(E) expects to reduce the defects because R32 has high operating pressure, large latent heat and high thermal conductivity. In order to prove the possibility, heat transfer coefficients during condensation and evaporation were obtained experimentally and cycle simulations were carried out where heat transfer degradation of refrigerant mixture was estimated with the experimental data. An equivalent performance with conventional refrigerant was obtained by the simulation.

1. INTRODUCTION

Chlorofluorocarbons (CFCs) and hydrochlorofluorocarbons (HCFCs) were prohibited in developed countries because of their high ozone depletion potential (ODP). Although hydrofluorocarbons (HFCs) have zero-ODP and they are widely used as refrigerants of air-conditioners, refrigerators and heat pumps, they are led into regulation because of their high global warming potential (GWP). Under these circumstances, hydrofluoroolefins (HFOs), such as R1234yf and R1234ze(E) which have low GWP are getting attention as alternative refrigerants of HFCs. GWPs of R1234yf and R1234ze(E) are 4 and 6, respectively. R1234yf is especially expected as a refrigerant of mobile air-conditioners because its thermophysical properties are very close to R134a which is presently used. R1234ze(E) has already been manufactured as a cover gas. Application of R1234ze(E) in turbo refrigerators is being tested. They would be the closest to commercialization.

In the present study, we focus on R1234ze(E) though it has some defects which are low operating pressure and low latent heat when it is used in room and packaged air-conditioners. These defects cause large volume of compressor and low coefficient of performance (COP). Mixing R32 into R1234ze(E) is one of solutions to reduce the defects because R32 has high operating pressure and superior properties which are large latent heat and high thermal conductivity. R32 is a HFC and its GWP is 675 which is comparably lower than other HFCs. Mixture of R1234ze(E) and R32 may give an acceptable GWP.

In our previous study (Onaka *et al.*, 2011), cycle analyses of refrigerant mixtures of CO₂/DME and R1234ze(E)/R32, pure refrigerant of them, and some conventional refrigerants have been carried out and the cycle characteristics was clarified. The heat transfer between refrigerant and heat sink/source water was considered by giving thermal conductance of condenser and evaporator. An example of simulation result of R1234ze(E)/R32 by Onaka *et al.* (2011) is shown in Figure 1. Figure 1(a) indicates the variation of COP_h and Figure 1(b) the variation of irreversible losses. The solid line in Figure 1(a) is the COP_h of R410A which is shown for comparison. The COP_h has the maximum value at around R1234ze(E)/R32 (65/35 mass%) and it is higher than that of R410A. In Figure 1(b), the vertical axial indicates the ratio of irreversible loss L and heating capacity (h_1-h_2). The variation of total irreversible loss corresponds to the variation of COP_h. Quantities of the irreversible losses are larger for heat exchangers, condenser and evaporator. From these results, it is inferred that appropriate evaluation of heat exchanger performance is important to obtain reliable results.

(a) Variation of COP_h with R32 mass fraction

(b) Variation of irreversible loss with R32 mass fraction

Figure 1: Cycle characteristics of refrigerant mixture R1234ze(E)/R32

Koyama *et al.* (2010) experimentally investigated the performance of R1234ze(E)/R32(50/50 mass%) mixture by using a heat pump system with R410A compressor. They reported that the COP_h of the mixture reduced only 7.5% of R410A.

In the present study, heat transfer coefficients during condensation and evaporation are obtained experimentally for pure refrigerants, R1234ze(E) and R32, and their mixture. The thermal conductance of condenser and evaporator are estimated from the experimental data and the cycle simulations are carried out by using the estimated thermal conductance. For the comparison, the heat transfer coefficient of R410A is measured and the cycle simulation is conducted.

2. EXPERIMENTAL APPARATUS

Experimental apparatus which is a vapor compression heat pump cycle consists of an inverter controlled compressor, a test condenser, a sub cooler, an expansion valve, and a test evaporator. Heat source water kept at a constant temperature is supplied to the test sections from a heat source unit with constant flow rate. The refrigerant pressure and flow rate are controlled by varying the rotating speed of compressor, opening the expansion valve, and adjusting the by-path valve. The mass flow rate of refrigerant is measured by a Coriolis mass flow meter.

Figure 2 shows schematic diagram of the test section. The test section was horizontally installed double tube heat exchanger. The total length of the test section is 5.81 m where the effective heat transfer length is 3.6 m and a U-bend exists in the test section. Refrigerant flows inside an inner tube and cooling water flows through the annular space in a counter current. In order to measure quasi-local heat transfer, the annular channel is divided into 12 tube subsections with each subsection length 300 mm. The inner tube is the smooth test tube made of copper and of 4.35 mm inner diameter and 6.35 mm outer diameter. The outer tube is made of poly-carbonated resin and of 9 mm inner diameter 13 mm outer diameter.

Temperatures of the heat source water are measured at inlet and outlet of each subsection by copper-constantan (T-type) thermocouples calibrated in uncertainty of $\pm 0.013^\circ\text{C}$. At the central position of each subsection, outside wall temperature of the inner tube is measured with four T-type thermocouples which are distributed circumferentially at the top, left, bottom and right sides of the tube where the thermocouples were calibrated in uncertainty of $\pm 0.013^\circ\text{C}$. Refrigerant temperature and pressure drop in the test tube are measured at every 0.92 m length from the entrance to the exit. Refrigerant temperature measured by K-type thermocouple calibrated in uncertainty of $\pm 0.061^\circ\text{C}$. Accuracies of the measurements of the absolute pressure and the pressure difference were within $\pm 1.8\text{kPa}$ and $\pm 0.15\text{kPa}$. Flow rates of the refrigerant and heat source water were measured within the accuracy of $\pm 0.071\%$ and $\pm 0.21\%$, respectively. A small amount of refrigerant (liquid) is sampled after the sub cooler by operating the valve of the gas chromatograph; as it passes through the capillary tube, the liquid becomes vapor due to the change of

pressure in the capillary tube. Then, the concentration of the mixture refrigerant is measured by the gas chromatograph with estimated ± 0.002 kg/kg. The heat balance between refrigerant and water of most of the test runs agreed within $\pm 10\%$ error. By using above data, an estimate for uncertainty of heat transfer coefficient was around 8%.

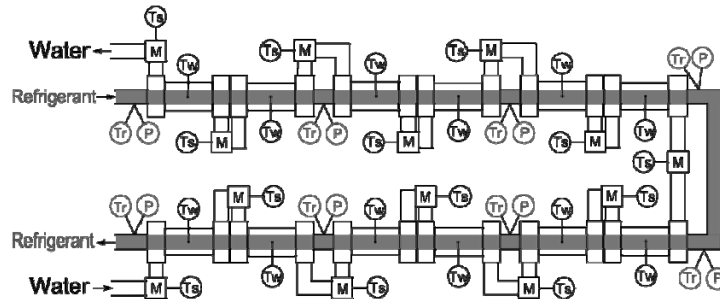


Figure 2: Schematic diagram of Test Section, condenser and evaporator

3. DATA REDUCTION

Heat transfer rates of refrigerant in the condenser and evaporator, Q_{RC} and Q_{RE} , are obtained from enthalpy change from the test section inlet to outlet, Δh_{RC} and Δh_{RE} , with the following equation.

$$Q_{R(C \text{ or } E)} = W_R \Delta h_{R(C \text{ or } E)} \quad (1)$$

Where, W_R indicates the flow rate of refrigerant and the subscript (C or E) becomes C for condenser and E for evaporator. The refrigerant enthalpy is calculated by REFPROP 9.0 (Lemmon *et al.*, 2010). On the other hand, the heat transfer rates of heat sink/source water side, Q_{SC} and Q_{SE} , are calculated with the flow rate W_S and temperatures measured at the test section inlet and outlet, T_{SI} and T_{SO} .

$$Q_{S(C \text{ or } E)} = W_{S(C \text{ or } E)} C_{PS} |T_{SI} - T_{SO}|_{(C \text{ or } E)} \quad (1)$$

C_{PS} is the specific heat capacity of water. Heat balances in the condenser and evaporator are expressed with following equation.

$$\eta_{HB(C \text{ or } E)} = Q_{R(C \text{ or } E)} / Q_{S(C \text{ or } E)} \quad (1)$$

The heat transfer rates in each subsection, ΔQ_{SC} and ΔQ_{SE} , are calculated with the measured subsection inlet and outlet temperature, T_{Si} and T_{So} .

$$\Delta Q_{S(C \text{ or } E)} = W_{S(C \text{ or } E)} C_{PS} |T_{Si} - T_{So}|_{(C \text{ or } E)} \quad (1)$$

Heat flux of the subsection is given with ΔQ_S and η_{HB} as follows.

$$q_{R(C \text{ or } E)} = (\Delta Q_S \eta_{HB})_{(C \text{ or } E)} / (\pi d_i \Delta z) \quad (1)$$

Where, d_i and Δz are inner diameter and length of subsection. The heat flux of each subsection is modified by the heat balance factor in order to avoid large inconsistent at exit sections. The representative inner wall temperature at the middle length of each subsection of the test tube is obtained by

$$T_{wi} = T_{wo} \pm \frac{\Delta Q_S \eta_{HB} \ln(d_o / d_i)}{2\pi \lambda_{co} \Delta z} \quad (1)$$

Where, T_{wo} is average outer wall temperature calculated from measurement point of top, right, bottom and left. λ_{co} is thermal conductivity of the copper tube. \pm is + for condenser and – for evaporator. The quasi-local heat transfer coefficient of each subsection during the condensation and evaporation are defined as

$$\alpha_{\text{exp}(C \text{ or } E)} = \frac{q_{R(C \text{ or } E)}}{|T_b - T_{wi}|} \quad (1)$$

T_b is the bulk temperature that is the equilibrium temperature of the refrigerant. Each subsection inlet and outlet bulk enthalpies are calculated by following equation:

$$h_{bo} = h_{bi} \mp \frac{q_R \pi d_i \Delta z}{W_R} \quad (1)$$

Where, \mp is – for condenser and + for evaporator. The thermodynamic equivalent quality x is given by

$$x = \frac{h_b - h_l}{h_v - h_l} \quad (1)$$

where, the enthalpies of saturated liquid and vapor, h_l and h_v , of pure fluids are determined with the aid of REFPROP 9.0 (Lemmon et al. 2010). The enthalpies, h_l and h_v , of mixture are calculated with the REFPROP 9.0 installed mixing parameters which were suggested by Koyama *et al.* (2010).

4. EXPERIMENTAL RESULTS OF CONDENSATION AND EVAPORATION

4.1 Experimental Conditions

Experimental conditions of condensation and evaporation are shown in Table 1 and 2. Pure refrigerant R1234ze(E) and R32, and their mixture with mass fraction of 55mass%R1234ze(E) and 45mass%R32 were tested. For comparison, the heat transfer coefficients of R410A were also measured.

Table 1: Experimental conditions of condensation

Refrigerant	Saturation temperature T_{sat} or T_{ave} [°C]	Mass flux G [kg m ⁻² s ⁻²]	Number of data n
R32	30, 35, 40	204-412	100
R1234ze(E)	30, 35, 45	147-399	75
R1234ze(E)/R32 (55/45 mass%)	30, 35, 45	170-404	160
R410A	40	215-394	32

Table 2: Experimental conditions of evaporation

Refrigerant	Saturation temperature T_{sat} or T_{ave} [°C]	Mass flux G [kg m ⁻² s ⁻²]	Heat flux q [kW m ⁻²]	Number of data n
R32	30, 35, 40	204-412	17.5-120	56
R1234ze(E)	30, 35, 45	147-399	8.3-51.1	34
R1234ze(E)/R32 (55/45 mass%)	30, 35, 45	170-404	12.3-41.1	65
R410A	40	215-394	18.2-72.6	46

For the mixture, the average temperature T_{ave} of dew and boiling points at the condensing pressure was set as the experimental condition.

4.2 Experimental Results

Figure 3 shows condensation heat transfer coefficients α_{exp} of the pure refrigerants R1234ze(E), R32, R410A and a mixture R1234ze(E)/R32(55/45 mass%). Figure 3(a) indicates the variation of local heat transfer coefficients with wetness ($1-x$) under the condition of saturation temperature $T_{ave}=40^{\circ}\text{C}$ and mass velocity $G=250\text{ kg m}^{-2}\text{ s}^{-1}$. Similar to typical condensation behavior, all the local heat transfer coefficients decrease with processing the condensation. The heat transfer coefficient of R32 is the highest in all the condensation area and those of R1234ze(E), R410A and the mixture R1234ze(E)/R32(55/45 mass%) show comparable values though R1234ze(E) and the mixture R1234ze(E)/R32 tend to be higher than R410A in this condition.

The average heat transfer coefficients $\bar{\alpha}$ of these refrigerants are shown in Figure 3(b) where the abscissa is the mass velocity G . In the experiments, refrigerant entered into the test section as a superheated vapor and flow out as a subcooled liquid. The average heat transfer coefficients shown in Figure 3(a) were obtained by averaging in condensing region. All the average heat transfer coefficient increase with the mass velocity increase. R32 shows the highest heat transfer coefficient in all the mass velocity condition. The average heat transfer coefficient of R1234ze(E) is higher than R410A and a rapid increase is observed around mass velocity of $350\text{ kg m}^{-2}\text{ s}^{-1}$. The average heat transfer coefficient of R1234ze(E)/R32(55/45 mass%) is close to that of R410A. The average heat transfer coefficient at mass velocity of $G=300\text{ kg m}^{-2}\text{ s}^{-1}$ is summarized in Table 3. Ratios to R410A are also indicated.

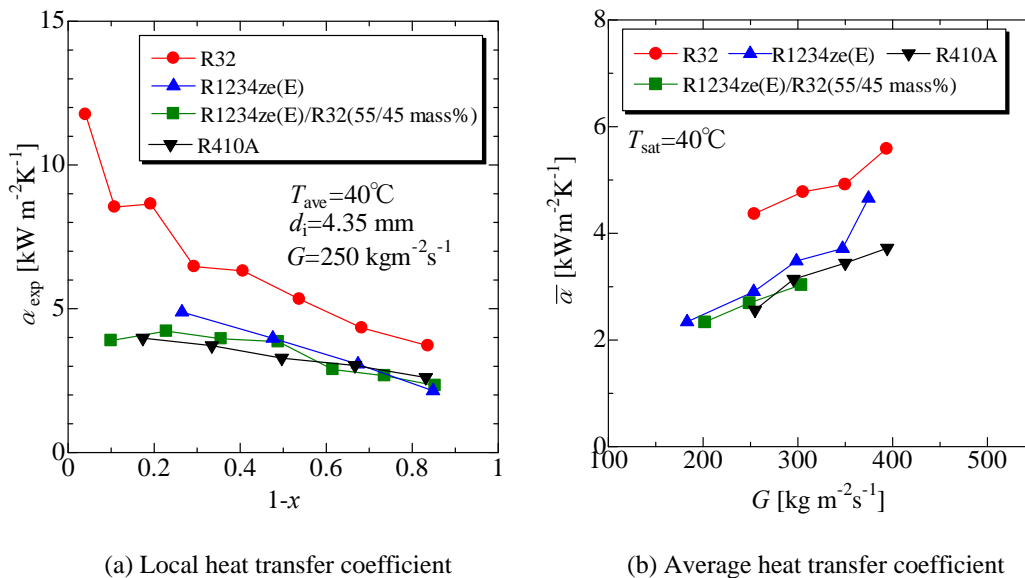


Figure 3: Condensation heat transfer coefficient

Table 3: Ratio of condensation heat transfer coefficient for R410A

Refrigerant	Average heat transfer coefficient $\bar{\alpha}$ [kW m ⁻² K ⁻¹]	Ratio to R410A $\bar{\alpha} / \bar{\alpha}_{R410A}$
R32	4.8	1.5
R1234ze(E)	3.5	1.1
R1234ze(E)/R32 (55/45 mass%)	3.0	1.0
R410A	3.1	-

Figure 4 shows evaporation heat transfer coefficients α_{exp} of the pure refrigerants R1234ze(E), R32, R410A and a mixture R1234ze(E)/R32(55/45 mass%). Figure 4(a) indicates the variation of local heat transfer coefficients with quality x under the condition of saturation temperature $T_{\text{ave}}=10^\circ\text{C}$ and mass velocity $G=300 \text{ kg m}^{-2} \text{ s}^{-1}$. Similar to typical evaporation behavior, all the local heat transfer coefficients increases with processing the evaporation and the dryout occurs at around $x=0.8$. The heat transfer coefficient of R32 is the highest in all the evaporation area and that of R410A is the second. R1234ze(E) and R1234ze(E)/R32(55/45 mass%) have comparable heat transfer coefficient and the lowest among the tested refrigerants. The behavior of high heat transfer of R410A in evaporation differs from the condensation explained above where the heat transfer coefficient of R1234ze(E) is slightly higher than that of R410A. This difference might be caused by effects of nucleate boiling.

The average evaporation heat transfer coefficients $\bar{\alpha}$ of these refrigerants are shown in Figure 4(b) where the abscissa is the mass velocity G . For all the experiments, refrigerant entered into the test section as a saturated two phase flow and flow out as a superheated vapor. The average heat transfer coefficients shown in Figure 4(a) were obtained by averaging the evaporation region which is from the inlet to before the dryout point. All the average heat transfer coefficient increase with the mass velocity increase. R32 shows the highest heat transfer coefficient in all the mass velocity condition. The average heat transfer coefficients of R1234ze(E) and R1234ze(E)/R32(55/45 mass%) are almost same. The average evaporation heat transfer coefficient and the ratio to R410A at mass velocity of $G=300 \text{ kg m}^{-2} \text{ s}^{-1}$ are summarized in Table 4.

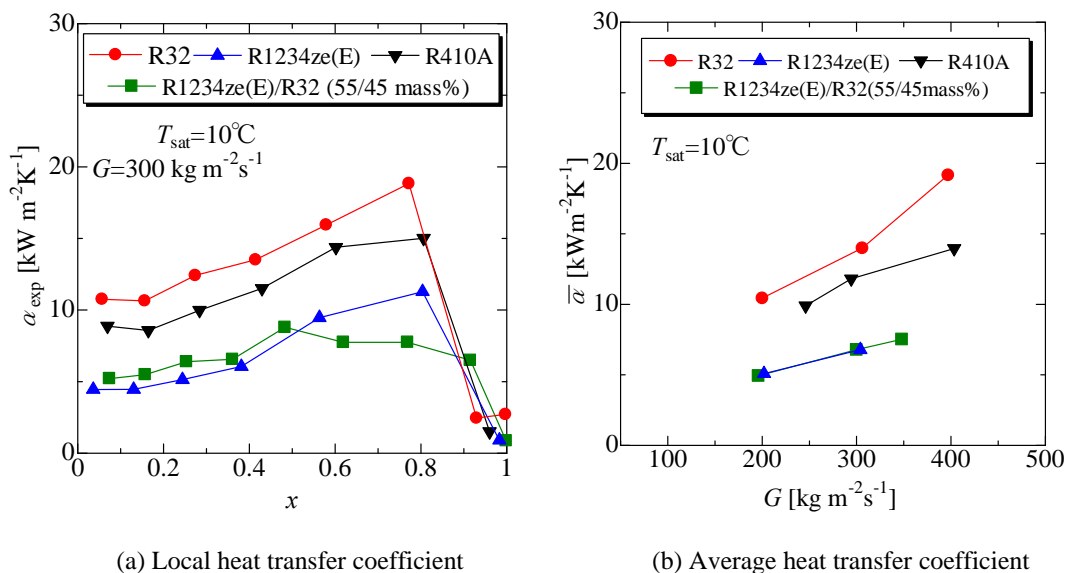


Figure 4: Condensation heat transfer coefficient

Table 4: Ratio of evaporation heat transfer coefficient for R410A

Refrigerant	Average heat transfer coefficient $\bar{\alpha}$ [kW m ⁻² K ⁻¹]	Ratio for R410A $\bar{\alpha} / \bar{\alpha}_{\text{R410A}}$
R32	14.0	1.2
R1234ze(E)	6.8	0.57
R1234ze(E)/R32 (55/45 mass%)	6.8	0.57
R410A	11.8	-

5. CYCLE SIMULATION WITH ESTIMATED THERMAL CONDUCTANCE

As explained in INTRODUCTION, appropriate estimation of thermal conductance is important to analyze the cycle performance of refrigerant mixture. Although in our previous study (Onaka *et al.*, 2011) where the thermal conductance is given as a constant parameter, the optimum COP_h was obtained at a certain concentration of refrigerant mixture, the heat transfer degradation of the refrigerant mixture would prevent the improvement. As shown in our experiment, heat transfer coefficients are different in each refrigerant. For more reliable simulation, appropriate thermal conductance has to be given to condenser and evaporator.

In order to give the proper thermal conductance, the experimental results explained in previous chapter are used to calculate the thermal conductance KA of condenser and evaporator with the following equation.

$$KA = \frac{\pi L}{\frac{1}{\alpha_R d_i} + \frac{1}{\alpha_S d_o}} \quad (1)$$

Where, α_R is the heat transfer coefficient of refrigerant, α_S is the heat transfer coefficient of the heat sink/source water, L is the length of heat exchanger, d_i is inner tube inside diameter, and d_o is inner tube outside diameter. α_R is obtained from the experimental results and α_S is calculated with Dittus-Boelter correlation. The estimated thermal conductance of each refrigerant is given in Table 5.

Table 5: Thermal conductance of smooth tube (at $G=300 \text{ kg m}^{-2}\text{s}^{-1}$)

Refrigerant	Average thermal conductance of condenser KA [kW/K]	Average thermal conductance of evaporator KA [kW m ² K ⁻¹]
R32	0.232	0.331
R1234ze(E)	0.195	0.262
R1234ze(E)/R32 (55/45 mass%)	0.179	0.262
R410A	0.183	0.316

By using the thermal conductance, cycle simulations have been conducted where the simulation method is similar with Onaka *et al.* (2011). The simulation conditions are shown in Table 6. The heating capacity at the condenser, heat sink/source water temperatures at the condenser and evaporator inlet and outlet are given as a operating condition.

Table 6: Cycle simulation condition

Q_{RC} [kW]	3.0
T_{SIC} [°C]	20
T_{SOC} [°C]	65
T_{SIE} [°C]	20
T_{SOE} [°C]	5

In Figure 5, variations of COP_h with operating pressure of condenser are plotted. For each refrigerant, COP_h has a maximum at certain pressure. The optimum values of COP_h and pressure at which the maximum value is reached are different in each refrigerant. The optimum COP_h of R32 is the highest and the second is R1234ze(E)/R32(55/45 mass%).

Variation of COP_h with R32 mass fraction is shown in Figure 6. Calculated results are plotted with symbols and a linear line connecting both the pure refrigerant is also plotted. COP_h of R1234ze(E) is lower than R32 though they were comparable value in Figure 1(a). COP_h of R1234ze(E)/R32(55/45 mass%) is higher than R1234ze(E) but it is lower than the linear line. This deterioration of COP_h is caused by the heat transfer degradation.

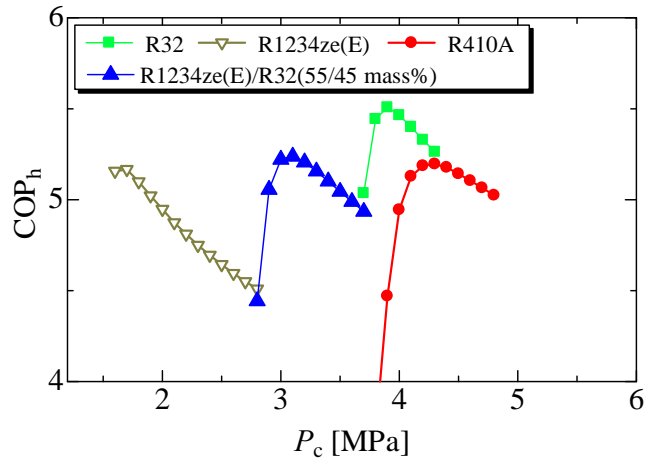


Figure 5: Variation of COP_h with operation pressure of condenser P_c

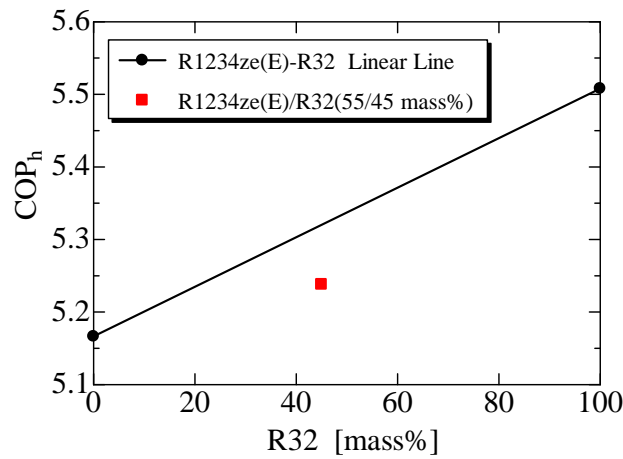


Figure 6: Variation of COP_h with R32 mass fraction

Because microfin tubes are used in most of the heat exchanger and heat transfer is enhanced, cycle simulations in which a microfin tube heat exchanger was supposed were carried out. In order to simulate the microfin tube, the heat transfer coefficients of condensation and evaporation of smooth tube shown in Tables 3 and 4 were multiplied by 1.3. The calculated thermal conductance of condenser and evaporator is indicated in Table 7.

Table 7: Thermal conductance estimated for microfin tube (at $G=300 \text{ kg m}^{-2}\text{s}^{-1}$)

Refrigerant	Average thermal conductance of condenser [kW/K]	Average thermal conductance of evaporator [kW m ⁻² K ⁻¹]
R32	0.263	0.351
R1234ze(E)	0.226	0.289
R1234ze(E)/R32 (55/45 mass%)	0.209	0.289
R410A	0.213	0.338

For the cycle assumed with microfin heat exchanger, variation of COP_h with R32 mass fraction is shown in Figure 7. Calculated results are plotted with symbols and a linear line connecting both the pure refrigerant is also plotted. COP_h of R1234ze(E)/R32(55/45 mass%) is higher than R1234ze(E) and it is on the linear line. The heat transfer enhancement is more sensitive for the mixture.

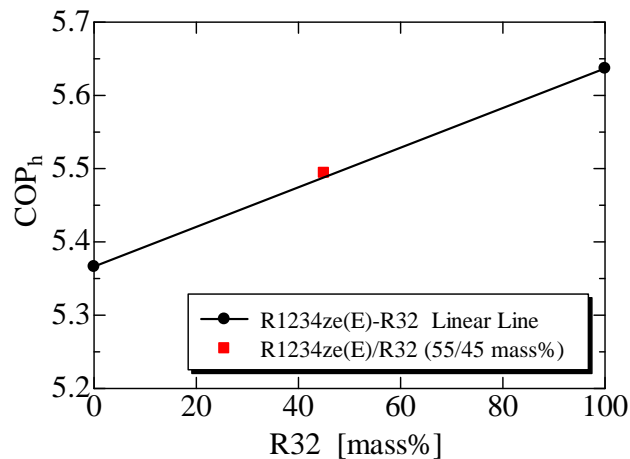


Figure 7: Variation of COP_h with R32 mass fraction for estimated thermal conductance of microfin tube

6. CONCLUSION

Cycle analyses of pure refrigerants R1234ze(E), R32, R410A and a mixture R1234ze(E)/R32(55/45 mass%) have been conducted in order to investigate a possibility of refrigerant mixture R1234ze(E)/R32. The thermal conductance used in the analyses was estimated with experimentally obtained condensation and evaporation heat transfer coefficient of smooth tube. In the present simulation condition, the obtained COP_h of R1234ze(E)/R32(55/45 mass%) is between those of R32 and R1234ze(E) and it is higher than that of R410A. However, the COP_h of the mixture is lower than a value linearly interpolated of both the pure refrigerants. On the other hand, a cycle simulation where the thermal conductance is estimated for microfin tube gives a result that the COP_h of the mixture is comparable to the linearly interpolated value. It is inferred that the heat transfer enhancement is important to use refrigerant mixtures.

REFERENCES

- Koyama, S., Takata, N., Fukuda, S., (2010), "Drop-in Experiments on Heat Pump Cycle Using HFO-1234ze(E) and Its Mixtures with HFC-32.", *International Refrigeration and Air Conditioning Conference at Purdue*, 2514.
- Lemmon, E.W., Huber, M.L., McLinden, M.O, (2010), "REFPROP: Reference Fluid Thermodynamic and Transport Properties", NIST Standard Database, Version 9.0.
- Onaka, Y., Miyara, A., Tsubaki, K., Koyama, S., 2011, Cycle Evaluation of Refrigerant Mixtures of CO_2 /DME and HFC-32/HFO-1234ze(E), *Proc. 23rd IIR Int. Conf. Refrigeration*, Prague, Czech Republic.